Structure and dynamics of chiral ferrielectric phases by deuteron NMR

J. Xu,[1] C. A. Veracini,[2] and Ronald Y. Dong[1,3]
[1]*Department of Physics and Astronomy, University of Manitoba, Winnipeg, MB, Canada R3T 2N2*
[2]*Departimento di Chemicae Chimica Industriale, Universita di Pisa, Via Risorgimento 35, 56126, Pisa, Italy*
[3]*Department of Physics and Astronomy, Brandon University, Brandon, MB, Canada R7A 6A9*
(Received 16 August 2005; published 12 January 2006)

The results of studying angular dependent spectral parameters in a magnetic field are reported in the chiral smectic *C* phases of a smectogen 1-methylheptyl 4′-(4-n-decyloxybenzoyloxy)-biphenyl-4-carboxylate. Our data provide direct evidence of a phase transition between two ferrielectric phases in this compound, viz. three-layer (SmC^*_{FiI}) and four-layer (SmC^*_{FiII}) superlattices. Simulation of spectral patterns of the methyl (C_{10}) deuterons obtained after an aligned sample is rotated by 90° in the magnetic field rules out the "clock model" for the three-layer and four-layer structures in these ferriphases. Instead, our data obtained under a magnetic field (9.4 T) seem to favor an "asymmetric clock model" for the interlayer packing. Interlayer jump rate is also obtained from the simulation of angular dependent spectra in these ferrielectric phases, and compared with those in the antiferroelectric SmC^*_A phase.

DOI: 10.1103/PhysRevE.73.011705 PACS number(s): 61.30.−v

I. INTRODUCTION

The discovery of antiferroelectric smectic *C* phase (SmC^*_A) in a liquid crystal (LC) [1] has led to many interesting tilted smectic structures (e.g., SmC^*_γ, SmC^*_α, and other subphases). This is a consequence of combining chirality (lack of mirror symmetry in molecules) and polarity [from lateral electric dipole(s) in molecules]. Numerous experimental studies [2–9] of chiral LC together with the development of a theoretical model which accounts for the relevant interlayer interactions have led to a typical phase sequence for these materials: SmC^*_α-SmC^*-SmC^*_{Fi2}-SmC^*_{Fi1}-SmC^*_A. Transition from the synclinic SmC^* to the low temperature SmC^*_A phase usually occurs via two intermediate subphases, because of frustrations between two very different helical superstructures. It is known that SmC^*_A has a two-layer periodicity with the molecules in neighboring layers having the same tilt angle θ_o with respect to the smectic planar normal, and a π difference between their azimuthal angles ϕ_i, while in a SmC^* phase ϕ_i varies continuously, but slightly from one layer to the next. The ferrielectric phases SmC^*_{Fi1} (or SmC^*_γ) and SmC^*_{Fi2} (or SmC^*_{AF}) show instead three-layer and four-layer periodicity, respectively [3,10,11]. It's also widely agreed at present that the clock model [12] or asymmetric clock model [13] is closer to the reality than the Ising model [14]. However, the disposition of molecules in a base unit for these ferriphases (see Fig. 2) has remained a subject of intense study for quite some time. A variety of experimental probes has been attempted to obtain the molecular disposition, including resonant x-ray [2–4,11], optical rotatory power [5–7], ellipsometry [8], and dynamic light scattering [9] studies. Deuterium NMR (DNMR) spectroscopy has been proven as a powerful technique to shed light on the structure, ordering, and dynamics of LC [15]. A recent work has demonstrated how the angular dependent deuteron spectral patterns can be used to extract interlayer jump diffusion rate in the SmC^*_A of a chiral LC [16]. Possible structural distortions by the NMR magnetic field can be satisfactorily treated [16–18]. Recently we have applied the same method to obtain the jump diffusion rate in the SmC^*_A phase of 1-methylheptyl
4′-(4-n-decyloxybenzoyloxy)-biphenyl-4-carboxylate
(sample 10B1M7) [19]. This molecule [see Fig. 1(a)] has been reported to show only one ferrielectric phase based on an optical study [20]. It would be of interest to verify this by means of NMR, even though the molecular arrangements in the ferriphases obtained under a high NMR magnetic field may not necessarily be the "ground state" structure. To the best of our knowledge, NMR technique has not been exploited to extract molecular arrangement information in ferrielectric phases. In this paper, angular dependent DNMR

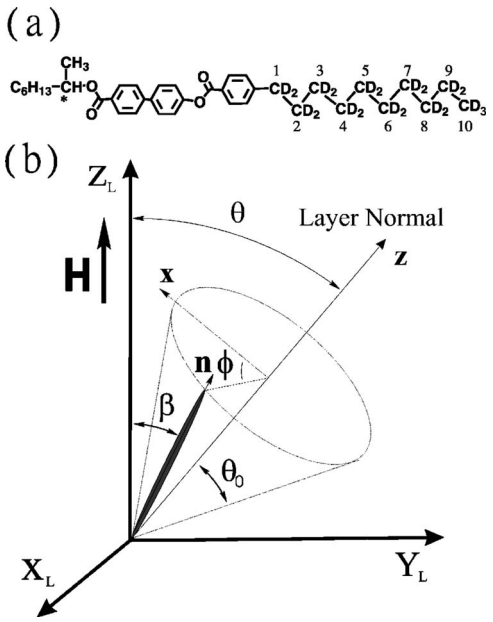

FIG. 1. (a) Molecular structure of a partially deuterated 10B1M7. (b) The geometry of a sample rotation experiment. **n** is the molecular director. (x,y,z) frame is fixed to the LC smectic layers.

spectral parameters are explored to extract the molecular structure and jump rates in the ferrielectric phase(s). In particular, the free induction decay (FID) intensity as a function of sample rotation angle is found to be a powerful means to distinguish between the Ising and distorted clock models. The paper is organized as follows. Section II outlines the necessary theory to describe the spectral patterns in the three- and four-layer ferrielectric phases. Section III gives a brief description of the experimental method, while Sec. IV contains the results and discussion. A brief summary is in the last section.

II. THEORY

The observed DNMR line shapes in SmC^*_{Fi} phases can be described as in the SmC^*_A phase [19] by a multisite jump problem, and the free precession evolution of the magnetization for one base unit (three or four layer) with azimuthal angle ϕ can be calculated by the Bloch-McConnell equation [21] $d\mathbf{M}/dt=\mathbf{\Lambda M}$, where $\mathbf{M}$ is a column vector with magnetization components M_i for the site i,

$$\mathbf{\Lambda}=\begin{pmatrix} -if(\phi-\varphi/2)-2\Omega & \Omega & 0 & \Omega \\ \Omega & -if(\phi+\varphi/2)-2\Omega & \Omega & 0 \\ 0 & \Omega & -if(\phi+\pi-\varphi/2)-2\Omega & \Omega \\ \Omega & 0 & \Omega & -if(\phi+\pi+\varphi/2)-2\Omega \end{pmatrix}, \tag{1}$$

$$\mathbf{\Lambda}=\begin{pmatrix} -if(\phi+\pi)-2\Omega & \Omega & \Omega \\ \Omega & -if(\phi-\varphi/2)-2\Omega & \Omega \\ \Omega & \Omega & -if(\phi+\varphi/2)-2\Omega \end{pmatrix}$$

for the SmC^*_{Fi2} and SmC^*_{Fi1} case, respectively, Ω is the probability of the molecule jumping from one layer to one of the two neighboring layers per unit time, φ is illustrated in Fig. 2 and $f(\phi)$ is the resonant frequencies for different sites given by [22]

$$f(\phi)=\pm\frac{3}{4}\pi\bar{\nu}_Q[3(\sin\theta\sin\theta_0\cos\phi+\cos\theta\cos\theta_0)^2-1], \tag{2}$$

with $\bar{\nu}_Q$ being a time-averaged nuclear quadrupolar coupling constant along the long molecule axis, and θ_0 the molecule tilt angle with respect to the normal of smectic layers. The geometry used for the angular dependent study is shown in Fig. 1(b). For an aligned sample produced by slow cooling from the isotropic phase, the helical pitch axis is along the external magnetic field. The magnetization formed [23] after a solid echo $(90^\circ_x-\tau-90^\circ_y-\tau)$ sequence [24] is

$$M(t)=Re[\vec{1}\cdot e^{\mathbf{\Lambda}(t+\tau)}(e^{\mathbf{\Lambda}\tau}\mathbf{M}^0)^*]. \tag{3}$$

Initially all sites are equivalent, and the initial condition $\mathbf{M}^0_{Fi2}=[\frac{1}{4},\frac{1}{4},\frac{1}{4},\frac{1}{4}]$ and $\mathbf{M}^0_{Fi1}=[\frac{1}{3},\frac{1}{3},\frac{1}{3}]$ are taken for convenience. The observed line shape is a linear superposition of magnetization from all the smectic layers within one pitch, and can be obtained by Fourier transform of the free induction decay calculated by

$$FID(t)=\int_0^{2\pi}\left(\frac{dz}{d\phi}\right)M(t)e^{-\sigma^2t^2/2}d\phi, \tag{4}$$

where $\exp(-\sigma^2t^2/2)$ is to account for the spectral line broadening with σ being a fitting parameter, $d\phi/dz$ describes the distribution of the azimuthal angle along the helical pitch (z) axis which accounts for possible distortions of the helical structure. From the spectra obtained at $\theta=90°$, a critical field $H_C>40$ T is estimated in both SmC^*_{Fi2} and SmC^*_A phases [19]. The intensity of echo maximum $I(\theta,2\tau)$ is simply given by Eq. (4) at $t=0$, i.e., $I(\theta,2\tau)=FID(0)$.

III. EXPERIMENTAL

The sample 10B1M7 was deuterated on the achiral chain [Fig. 1(a)] [19,25]. Based on our DNMR study, the SmC^*_{Fi} phase of 10B1M7 actually includes two subphases, and its relevant phase sequence by cooling is SmC^* (342 K) SmC^*_{Fi2} (335 K) SmC^*_{Fi1} (330.3 K) SmC^*_A. The sample was aligned and cooled to the desired temperature in the SmC^*_{Fi} phases for angular dependent studies. Deuterium spectral patterns were collected at 61.4 MHz on a Bruker Avance 400 system equipped with a Bruker high precision goniometer probe. Solid echo pulse sequence was used to generate all ^{2}H spectra and to give the echo maximum intensities at different rotation angles θ [see Fig. 1(b)]. The 90° pulse width was 3 μs. Typical number of scans needed to observe the FID or its Fourier transform was 128 and the recycle time between scans was 1.5 s. Our experiments showed that there was no observable field-induced sample reorientation or layer destruction in the studied θ region of $0°-90°$ for SmC^*_{Fi2} phase. The helical structure in SmC^*_{Fi1} phase was found to distort more easily than in SmC^*_{Fi2} and SmC^*_A phase by the NMR magnetic field. However, there was no sample reorientation or layer destruction found in SmC^*_{Fi1} phase up to 90°. This proves that the anticlinic order is far less sensitive to the

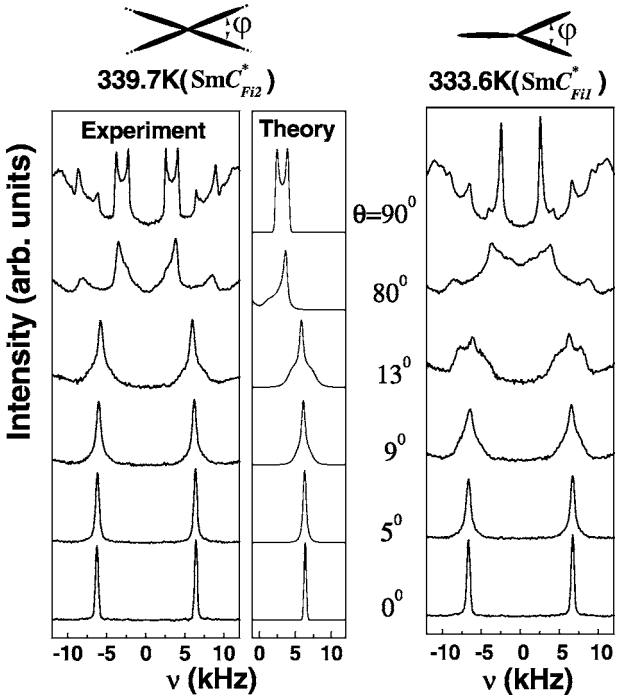

FIG. 2. Experimental angular dependent DNMR line shapes (only emphasize C_{10} methyl signal) in the SmC^*_{Fi1} (334.6 K) and SmC^*_{Fi2} (339.7 K) phase of 10B1M7. The molecule disposition in one repeat unit for these two phases are shown at the top. Also shown are simulated line shapes (positive halves only) for 339.7 K using Ω=5 kHz, $\bar{\nu}_Q$=8.2 kHz, θ_0=22.6°, φ=20°, and σ=1 kHz.

external magnetic field than synclinic ordering [16]. When measuring the angular dependent echo intensities, we focused on the C_{10} methyl deuterons whose spin-lattice relaxation times are the largest [26]. At the same time, the echo intensity did decay faster when $\bar{\nu}_Q/\Omega$ was larger [19]. Therefore, $\tau \geqslant 400$ μs was selected to avoid the complication introduced by the other deuterated sites, i.e., the measured echo intensities for θ angle between 3°–85° was mainly due to the C_{10} deuterons [19].

IV. RESULTS AND DISCUSSION

Typical angular dependent DNMR line shapes collected at τ=30 μs in the two phases are shown in Fig. 2. In the small rotation angle region, their line shapes are quite similar to those in SmC^*_A phase, i.e., the characteristic line shape of SmC^* phase with two singularities [17,22] is modulated by the interlayer diffusion of molecules to produce a line shape showing a single peak together with two shoulders [16]. The spectra of the SmC^*_{Fi1} phase show obvious structural distortions at high rotation angles, since the intensity of one edge singularity is much higher than that of the other, especially at θ=90°. The simulated line shapes in SmC^*_{Fi2} at 339.7 K using Eq. (4) and $dz/d\phi \approx$ constant are also plotted in Fig. 2 for direct comparison. From simulation of line shapes at different temperatures, the jump rates Ω have been obtained in the SmC^*_{Fi2} phase. These are plotted versus the reciprocal temperature along with those reported earlier [19] for the

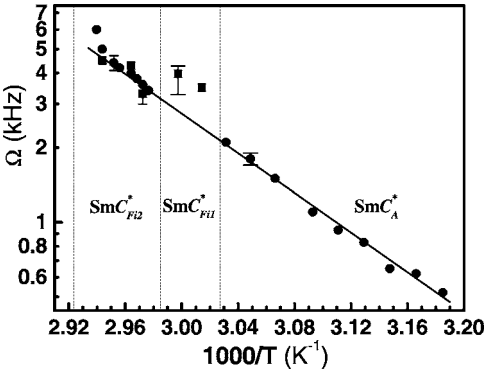

FIG. 3. Plot of interlayer jump rates Ω versus the reciprocal temperature obtained by fitting line shapes (●) in SmC^*_{Fi2} phase and the solid echo intensity curves(■) at different θ in both ferriphases. Ω in SmC^*_A phase (●) along with linear fitting curve (solid line) are reproduced here based on line-shape simulations [19]. Dashed lines denote phase transition temperatures between neighboring phases.

SmC^*_A phase in Fig. 3. It is clear from the figure that the activation energy for the jump process is same (ca. 78 kJ/mol) for the two anticlinic (four- and two-layer) phases. The theoretical spectra for θ=90° using different models, viz. different φ angles, using Eq. (4) are shown in Fig. 4(a) (SmC^*_{Fi1} phase) and Fig. 4(b) (SmC^*_{Fi2} phase), where typical values Ω=3 kHz, θ_0=21°, and $\bar{\nu}_Q$=10.5 kHz

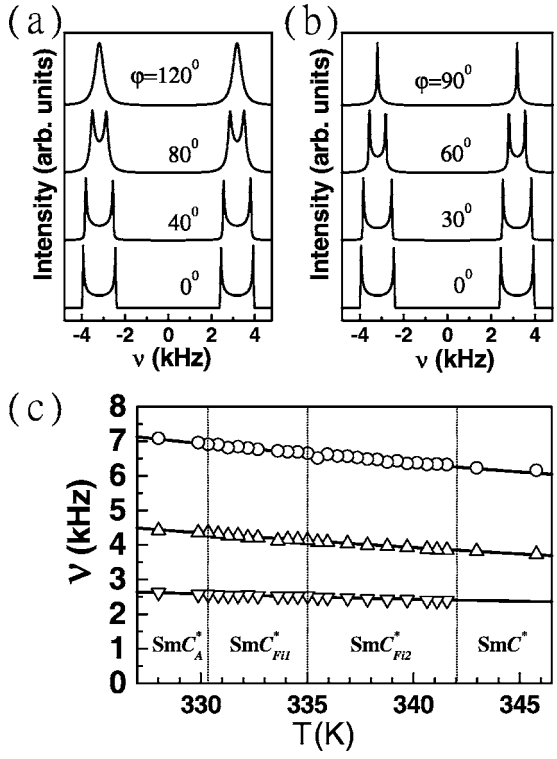

FIG. 4. Simulated line shapes using different azimuthal φ angles at rotation angle θ=90° for the three-layer SmC^*_{Fi1} phase (a) and the four-layer SmC^*_{Fi2} phase (b). (c)Plots of positive frequency at θ=0 (○) and frequencies of the two edge singularities seen at θ=90° (△ and ▽) versus the temperature. Solid lines denote fitted curves.

were used. When $\varphi=0$ for the Ising model, the line shapes are exactly same as those in SmC_A^* and SmC^* phases. As φ increases, the separation between two edge singularities decreases gradually. Eventually, the edge singularities collapse to a single peak for the perfect "clock model." Only a "distorted clock model" or "asymmetric clock structure" can explain the observed line shapes at $\theta=90°$ for these two ferriphases. The frequency at $\theta=0$ and the frequencies of the edge singularities seen at $\theta=90°$ are plotted versus the temperature in Fig. 4(c). There is no obvious frequency discontinuity across different studied chiral phases. In the Ising model, the three frequencies are same as those in the SmC^* and SmC_A^* phase, given by the following [22]:

$$\nu^{\pm} = \pm\frac{3}{4}\bar{\nu}_Q\left(1-\frac{3}{2}\sin^2\theta_0\right)\ (\theta=0°),$$

$$\nu_1^{\pm} = \pm\frac{3}{8}\bar{\nu}_Q, \quad \nu_2^{\pm} = \pm\frac{3}{4}\bar{\nu}_Q\left(1-\frac{3}{2}\cos^2\theta_0\right)(\theta=90°). \tag{5}$$

Solid lines in Fig. 4(c) are globally fitted curves using Eq. (5) by assuming that θ_0 has a second order polynomial temperature dependency and $\bar{\nu}_Q$ has a linear temperature dependency, leading to

$$\theta_0 = 20.65 + 0.128(T-T_c) + 4.30\times10^{-3}(T-T_c)^2,$$

$$\bar{\nu}_Q = 10.24 + 0.112(T-T_c), \quad T_c = 342\ \text{K}. \tag{6}$$

The good agreement between the calculated and experimental data does not preclude a small nonzero φ, since the edge singularities at $\theta=90°$ are not sensitive to small φ values (e.g., frequency shift about 2% at $\varphi=33°$ in SmC^*_{Fi1} phase, and at $\varphi=27°$ in SmC^*_{Fi2} phase). To demonstrate that the asymmetric clock structure is a proper description of the two ferrielectric phases in 10B1M7, accurate φ determination can only be extracted from the angular dependent echo intensity curve.

The measured echo intensities $I(\theta,2\tau)$ normalized by the intensity at $\theta=0$, $I(0,2\tau)$ for a typical temperature in the two ferriphases, and two τ values are plotted as a function of θ in Fig. 5. The echo intensity at $\theta=0$, $I(0,2\tau)$ was taken as an adjustable parameter. Thus, four parameters $I(0,2\tau)(\tau=400\ \mu s)$, $I(0,2\tau)(\tau=600\ \mu s)$, Ω, and φ were used to simultaneously fit the two curves with $\bar{\nu}_Q$ and θ_0 calculated from Eq. (6). In SmC^*_{Fi1} phase, the fitting is only limited to small θ angles, i.e., $\leqslant 25°$, to avoid tedious calculations due to the magneto-induced distortion of the helical structure. For small angles, the distortion is small and $dz/d\phi \approx$ constant was used. It is seen that the theoretical curves are in excellent agreement with the experiment. Fitting the angular dependent echo intensities at three temperatures in SmC^*_{Fi2} phase yields $\varphi=22\pm3°$ (339.7 K), $19\pm3°$ (337.4 K), $25\pm3°$ (336.4 K), and two temperatures in SmC^*_{Fi1} phase $\varphi=22\pm5°$ (331.7 K), and $23\pm5°$ (333.6 K), as well as their corresponding jump rates Ω, shown also in Fig. 3. Thus, the φ angle appears to be identical within experimental uncertainties in these ferriphases. This is consistent with the conclusion obtained by x-ray technique [2]. Even the angle φ compares well with those of the chiral LC MHDDOPTCOB [2,8]. The derived Ω using echo intensities in the SmC^*_{Fi2} compares well with those obtained above by line shape simulations [Eq. (4)]. The self-diffusion constant is related to the interlayer jump rate by $D_{\|}=4L^2\Omega/\pi^2$ (L is the smectic layer thickness) under the assumption that molecules can freely diffuse to the two neighboring layers [19]. The temperature-dependent layer thickness L for this compound has been measured using x-ray method [27]. It is found that the layer thickness is only slightly temperature dependent in the SmC^*_{Fi} phases. The average value $L=3.5$ nm can be used to estimate the diffusion constant. Typical calculated values in the two phases are $D_{\|}(337.4\ \text{K})=2.1\times10^{-14}\ \text{m}^2/\text{s}$ and $D_{\|}(331.7\ \text{K})=1.7\times10^{-14}\ \text{m}^2/\text{s}$. The self-diffusion or jump rate is a thermally activated process in SmC^*_{Fi2} phase except the pretransitional behavior near the transition to the ferroelectric phase. The sudden change of self-diffusion between synclinic and anticlinic phase was also observed by traditional self-diffusion measurements on the same sample [27], though their values are significantly higher. It is interesting to note that the Ω values in the SmC^*_{Fi1} phase do not fall on the solid line in Fig. 3, indicating a deviation from the behaviors of its two neighboring phases. To obtain Ω by fitting line shapes in SmC^*_{Fi1} phase is harder due to the distortion of

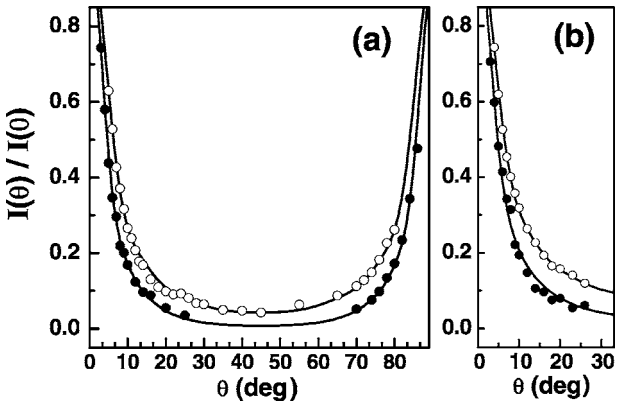

FIG. 5. Experimental echo intensities $I(\theta)$ versus the rotation angle θ for $\tau=400\ \mu s$ (○) and $\tau=600\ \mu s$ (●) along with fitting curves (solid lines) at (a) 339.7 K in SmC^*_{Fi2} phase and (b) 331.7 K in SmC^*_{Fi1} phase. The intensities are normalized by the intensity at $\theta=0$, $I(0)$, which is treated as an adjustable parameter (see text).

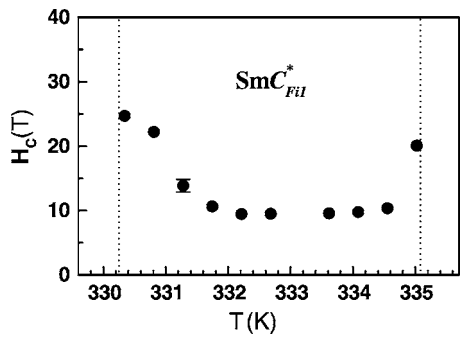

FIG. 6. The temperature dependent critical field H_c in SmC^*_{Fi1} phase (●). The transition temperatures are denoted by dashed lines.

helical structure at large rotation angles. However, the critical field H_c can be obtained from the distorted spectra at $\theta = 90°$. The solitonlike distortion of the helical structure by the magnetic field in the chiral smectic phases can be explained by a simple Landau theory, which gives [16,17]

$$\left.\frac{dz}{d\phi}\right|_{\theta=90°} = \frac{\text{const}}{\sqrt{1-\kappa^2\cos^2\phi}}, \tag{7}$$

where κ is a fitting parameter, and is related to H_c by $H_c = H \cdot E(\kappa)/\kappa$ at $\theta = 90°$. Here $H = 9.4$ T and $E(\kappa)$ is the elliptical integral of the second kind. The critical field values in SmC^*_{Fi1} phase, plotted in Fig. 6, are obtained by fitting the spectra taken at $\theta = 90°$ and various temperatures using Eq. (4) and Eq. (7). It can be seen that there are sudden jumps of the critical field near the two phase transition temperatures of SmC^*_{Fi1} phase. It is noted that the interlayer jump rates in chiral ferriphases can not be obtained from experiments such as the resonant x-ray technique.

V. CONCLUSION

In summary, the local structure and dynamics of anticlinic smectic phases can be determined unambiguously, albeit in a high NMR field, from the angular dependent DNMR line shapes and solid echo intensities. At the same time, structural distortions under the external magnetic field can also be studied to find the critical field for unwinding the helices in the SmC^*_{Fi1} phase of 10B1M7. A monodeuterated sample will be useful for avoiding interference from other deuterated sites, thereby leading to more accurate φ and Ω values. This method also shows the potential for exploring other new phase structures that show large alternation of molecular tilt direction.

ACKNOWLEDGMENTS

The Natural Sciences and Engineering Council of Canada and Canada Foundation of Innovation are thanked for their financial support. CAV acknowledges the financial support of Italian MIUR.

[1] A. D. L. Chandani, E. Gorecka, Y. Ouchi, H. Takezoe, and A. Fukuda, Jpn. J. Appl. Phys., Part 1 **28**, L1265 (1989).
[2] A. Cady, J. A. Pitney, R. Pindak, L. S. Matkin, S. J. Watson, H. F. Gleeson, P. Cluzeau, P. Barois, A.-M. Levelut, and W. Caliebe, Phys. Rev. E **64**, 050702(R) (2001).
[3] P. Mach, R. Pindak, A.-M. Levelut, P. Barois, H. T. Nguyen, C. C. Huang, and L. Furenlid, Phys. Rev. Lett. **81**, 1015 (1998).
[4] M. Gorkunov, S. Pikin, and W. Haase, JETP Lett. **69**, 243 (1999).
[5] T. Akizuki, K. Miyachi, Y. Takanishi, K. Ishikawa, H. Takezoe, and A. Fukuda, Jpn. J. Appl. Phys., Part 1 **38**, 4832 (1999).
[6] I. Muševič and M. Škarabot, Phys. Rev. E **64**, 051706 (2003).
[7] M. Čepič, E. Gorecka, D. Pociecha, B. Žekš, and H. T. Nguyen, J. Chem. Phys. **117**, 1817 (2002).
[8] P. M. Johnson, D. A. Olson, S. Pankratz, T. Nguyen, J. Goodby, M. Hird, and C. C. Huang, Phys. Rev. Lett. **84**, 4870 (2000).
[9] D. Konovalov, H. T. Nguyen, M. Čopič, and S. Sprunt, Phys. Rev. E **64**, 010704(R) (2001).
[10] P. Mach, R. Pindak, A.-M. Levelut, P. Barois, H. T. Nguyen, H. Baltes, M. Hird, K. Toyne, A. Seed, and J. W. Goodby, Phys. Rev. E **60**, 6793 (1999).
[11] L. S. Hirst, S. J. Watson, H. F. Gleeson, P. Cluzeau, P. Barois, R. Pindak, J. Pitney, A. Cady, P. Johnson, and C. Huang, Phys. Rev. E **65**, 041705 (2002).
[12] M. Čepič and B. ŽekŠ, Mol. Cryst. Liq. Cryst. Sci. Technol., Sect. A **263**, 61 (1995).
[13] V. L. Lorman, Liq. Cryst. **20**, 267 (1996).
[14] A. Fukuda, Y. Takanishi, T. Isozaki, K. Ishikawa, and H. Takezoe, J. Mater. Chem. **4**, 997 (1994).
[15] R. Y. Dong, *Nuclear Magnetic Resonance of Liquid Crystals* (Springer-Verlag, Berlin, 1997).
[16] B. Zalar, A. Gregorovic, and R. Blinc, Phys. Rev. E **62**, R37 (2000).
[17] B. Zalar, A. Gregorovic, M. Simsic, A. Zidansek, R. Blinc, S. Keasr, and M. Neubert, Phys. Rev. Lett. **80**, 4458 (1998).
[18] J. Xu, C. A. Veracini, and R. Y. Dong, Chem. Phys. Lett. **416**, 47 (2005).
[19] J. Xu, C. A. Veracini, and R. Y. Dong, Phys. Rev. E **72**, 051703 (2005).
[20] J. Goodby, J. Patel, and E. Chin, J. Mater. Chem. **2**, 197 (1992).
[21] H. M. McConnell, J. Chem. Phys. **28**, 430 (1958).
[22] B. G. Wu and J. W. Doane, J. Magn. Reson. (1969-1992) **75**, 39 (1987).
[23] A. J. Vega and Z. Luz, J. Chem. Phys. **42**, 1615 (1965).
[24] J. H. Davis, K. R. Jeffrey, M. Bloom, M. I. Valic, and T. P. Higgs, Chem. Phys. Lett. **42**, 390 (1976).
[25] D. Catalano, M. Cavazza, L. Chiezzi, M. Geppi, and C. Veracini, Liq. Cryst. **27**, 621 (2000).
[26] R. Y. Dong, L. Chiezzi, and C. A. Veracini, Phys. Rev. E **65**, 041716 (2002).
[27] M. Cifelli, V. Domenici, and C. Veracini, Mol. Cryst. Liq. Cryst. Sci. Technol., Sect. A **429**, 167 (2005).